UDC 538.911

T. Inerbaev[1,2], P. Gavryushkin[3,4], K. Litasov[3,4], F. Abuova[1], A. Akilbekov[1]

[1]*L.N. Gumilyov Eurasian National University, Astana, Kazakhstan;*
[2]*Center for Computational Quantum Chemistry, South China Normal University, Guangzhou 510006, China;*
[3]*Sobolev Institute of Geology and Mineralogy Siberian Branch Russian Academy of Sciences, Russia*
[4]*Novosibirsk State University, Russia*
(E-mail: talgat.inerbaev@gmail.com)

P-V-T equation of state and thermoelastic properties of shortite $Na_2Ca_2(CO_3)_2$ from first principles

Theoretical study of structural, thermodynamic and dynamic properties of the double Na-Ca carbonate, shortite, was carried out with density functional theory. Local density approximation (LDA) and generalized gradient approximation in the Perdew-Burke-Ernzerh of (PBE) parameterization were used. Calculated structural and elastic properties exhibit typical behavior for both employed methods. At the same time, equation of state *P(V)* and bulk modulus, obtained by means of LDA and PBE are significantly different from each other at low pressure and high temperature. This difference is caused by dynamic instability of crystal which boundary calculated using LDA always lies at negative pressure region, while in the case of PBE calculations, this limit manifests itself at positive pressure resulting to features in equation of state *P(V)* and the bulk modulus behavior. Results indicate that accuracy of used theoretical method is critical for understanding the cause of shortite lattice instability at low pressure and sufficiently high temperature.

Keywords: Na-Ca carbonates; first principles density functional calculation; lattice dynamics; elastic moduli; stability.

1. Introduction

Double Na-Ca carbonates is relatively rare and scarcely investigated class of compounds. Up to now only 5 compounds of this class are known: $Na_2Ca(CO_3)_2$ (mineral nyerereite) [1], $Na_2Ca_2(CO_3)_3$(mineral shortite) [2], $Na_2Ca_3(CO_3)_4$ [3, 4], $Na_2Ca_4(CO_3)_5$, and $Na_4Ca(CO_3)_3$ [5]. Among these five compounds crystal structures are known for only first three. They crystallize in acentric space groups: $Na_2Ca(CO_3)_2$- $P2_1ca$ [6], $Na_2Ca_2(CO_3)_3$ – $Amm2$ [2], and $Na_2Ca_3(CO_3)_4$ – Pn [3]. First and last compounds are pseudocentric and relatively small atomic shifts transform them into centric structures. Only $Na_2Ca_2(CO_3)_2$ is truly acentric, even atomic shifts on distances up to 0.4 Å does not transform it into centrosymmetric structure (pseudosymmetry determination with higher tolerance is problematic). This acentricity indicate on the perspective of its use in laser optics for second harmonic generation. This fact together with absence of any optical data on this compound was motivation for us to perform calculations presented in the article.

$Na_2Ca_2(CO_3)_2$ was found in nature as quite rare mineral shortite. However, due to the strong flux effect of alkaline carbonates on mantle rocks, shortite together with other Na-Ca carbonates attracts considerable attention in Earth sciences. Crystal structures, *P-T* stability fields and phase relations of Na-Ca carbonates are the object of intense experimental investigation [5]. This was the reason for us to perform additional calculations under high pressures and temperatures.

In this work we present the results of DFT calculations for the lattice constant, elastic constants, *P-V-T* equation of state, thermal expansion coefficient, limits of absolute stability and specific heat capacity of shortite. Results obtained with local density approximation (LDA) and generalized gradient approximation with Perdew-Burke-Ernzerhof (PBE) are compared.

2 Computation Details

2.1 Electronic structure caculations

Periodic density functional theory (DFT) calculations using projector-augmented wave (PAW) methods [7] with the LDA and PBE functionals were performed using the *ab initio* total energy and molecular dynamics program VASP (Vienna *ab initio* simulation program) [8, 9]. The numerical parameters were chosen to give an overall numerical error in the order of 1 meV per unit cell: the plane-wave cutoff energy was 1000 eV and integrations over Brillouin zone were performed on a k-points mesh with spacing between different k-points equal to 0.2 $Å^{-1}$ and centered on the Γ-point in reciprocal space. Such Brillouin zone sampling corresponds to taking into consideration of 105 k-points where 24 of them are irreducible. All atomic positions

in the uni tcell were relaxed by a conjugate-gradient algorithm while the lattice parameters were allowed to relax at the fixed unit cell volume. Vibrational frequencies were determined with afinite displacement method.

2.2 Lattice dynamics calculations

As starting point of our calculations, we adopted the experimental crystal structure of shortite [2] having the *Amm*2 space group (Fig. 1). The free energy F_{qh} of crystal in this model is calculated within the framework of lattice dynamics approach in the quasiharmonic approximation as

$$F_{qh} = E_0 + F_{vib}, \tag{1}$$

where E_0 is the ground state energy, F_{vib} is the vibrational contribution,

$$F_{vib} = \frac{1}{2}\sum\nolimits_j \hbar\omega_j + kT\sum\nolimits_j \ln\left[1-\exp\left(\frac{\hbar\omega_j}{kT}\right)\right], \tag{2}$$

where ω_j is the j-th frequency of crystal vibration.

In the quasiharmonic approximation the free energy of crystal has the same form as in the harmonic approximation but the structural parameters at fixed volume depend on the temperature. This dependence is determined self-consistently at calculation of the system's free energy. To obtain the equation of state *P(V)* at fixed temperature the expression $P = -\left(\partial F \big/ \partial V\right)_T$ was used. Bulk moduli were calculated from equation of state using expression $B = -V\left(\partial P \big/ \partial V\right)_T$. The thermal expansion coefficient α defined by

$$\alpha(T) = \frac{1}{V}\frac{dV}{dT}, \tag{3}$$

Constant volume and constant pressure heat capacities were calculated from Eq.1 as

$$C_v = -T\left(\frac{\partial^2 F}{\partial T^2}\right)_V, \tag{4}$$

$$C_p = C_v + \alpha^2 BVT, \tag{5}$$

where α, V, and B are the calculated linear thermal expansion coefficient, the equilibrium lattice constant, and the bulk modulus, respectively.

In literature, various exchange-correlation functionals were assessed for computing the structural, vibrational, and elastic properties of materials [10–14]. Unfortunately, there is no functional which is sufficiently accurate for all solids. It was shown that for the vibrational and thermodynamic properties LDA performs very well [12]. Comparison of theoretical and experimental results for set of various solids reveals that the LDA overestimation of the bulk moduli is about 15 % (too stiff) and the PBE underestimation is about 9 % (too soft), but considerable improvement over LDA [13, 14]. The ZPPE corrections, i.e. exclusion effect of zero-point lattice vibrations on the elastic moduli, would shift the corrected experimental values in the direction of LDA and worsen the agreement between experiment and PBE results [13].

2.3 Equation of state

The thermoelastic parameters for shortite were calculated using two conventional approaches for the temperature range above 298.15 K: a high-temperature (HT) EOS and a Mie-Grüneisen-Debye (MGD) EOS [15-17]. We follow Ref. [18] for formalism and abbreviations. For data at 298 K we used the Vinet-Rydberg (VR) EOS [19]:

$$P = 3K_T \frac{(1-\eta)}{\eta^2}\exp\left[1.5\left(K_T^{'}-1\right)(1-\eta)\right], \tag{6}$$

where $\eta = (V/V_0)^{1/3}$, K_T is the isothermal bulk modulus and K_T' is pressure derivative of K_T. The temperature effect on K_T and V_{0T} in HT EOS is expressed as:

$$K_T = K_{TO} + \left(\frac{\partial K_T}{\partial T}\right)_p (T - T_0), \tag{7}$$

$$V_{0T} = V_0 \exp\left[\int_{T_0}^{T} \alpha dT\right], \tag{8}$$

where $(\partial K_T / \partial T)_P$ is the temperature derivative of the bulk modulus, T_0 is reference temperature (298.15 K), and α is the volumetric thermal expansion at atmospheric pressure. The thermal expansion α is expressed as

$\alpha(T) = a_0 + a_1 T$. In this approach we optimize six parameters V_0, K_{T0}, K_T', $(\partial K_T/\partial T)_P$, a_0 and a_1, by fitting the *P-V-T* data to the HT-VR EOS.

The MGD formalism includes following expression for the thermal pressure ΔP_{th} in addition to static pressure at 300 K from the VR EOS:

$$\Delta P_{th} = \frac{\gamma}{V}\left[E_{th}(V,T,) - E_{th}(V,T_0)\right], \tag{9}$$

where γ is the Grüneisen parameter and E_{th} is the thermal energy, which can be calculated from the Debye model:

$$E_{th} = \frac{9nRT}{\left(\theta/T^3\right)}\int_0^{\theta/T}\frac{\xi^3}{e^{\xi}-1}d\xi, \tag{10}$$

where n is number of atoms in a formula unit (n = 12 for shortite), R is the gas constant, and θ is the Debye temperature. The volume dependence of θ and γ are described by following equations:

$$\theta = \theta_0 \exp\left[\frac{(\gamma_0 - \gamma)}{q}\right], \tag{11}$$

$$\gamma = \gamma_0\left(\frac{V}{V_0}\right)^q, \tag{12}$$

where q is dimensionless parameter. In this approach, the six fitted parameters are V_0, K_{T0}, K_T', γ_0, θ_0, and q.

3 Results and Discussion

3.1 Lattice constants

The experimental lattice constants include finite-temperature phonon effects (FTPE), and in Ref. [2] they were measured at room temperature. These experimental values are not directly comparable with the results of ground-state electronic structure calculations (static lattice). It was shown by Csonska et.al [13] that neglecting effects might invalidate any comparison of experiment and theory. In Ref. [13] zero-point phonon effects (ZPPE) were evaluated using stabilized jellium equation of state model introduced by Alchagirov et. al. [20]. In this work, we take into account both zero-point and finite temperature corrections to lattice parameters by neglecting or taking into consideration second temperature-dependent term in Eq. 2. In the case of static lattice, we completely neglected the contribution of F_{vib} in Eq. 1.

Experimental and theoretical lattice parameters of shortite are summarized in Table. Phonon uncorrected, i.e. static lattice PBE results, systematically overestimate lattice constants with relative error 1.2–1.5 %, while corresponding LDA data underestimate lattice constants with accuracy 2.1–4.4 %. Taking into account the phonon contribution to the free energy improves the accuracy of LDA calculated values of lattice constants and worsens the agreement between PBE results and experiment. Temperature dependence of shortite crystal lattice parameter at zero pressure is shown in Figure 3.

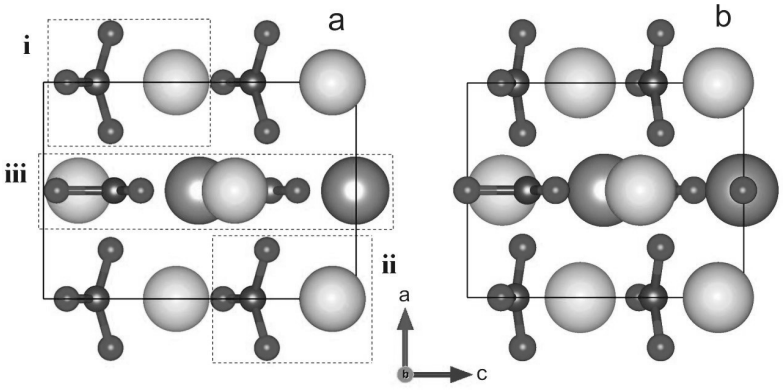

Figure 1. Shortite lattice relaxed using PBE functional at (a) P = 0 GPa and (b) 30 GPa. Dashed rectangulars shows atomic groups aligned along (i) (011), (ii) $\left(0\bar{1}1\right)$ and (iii) (001) directions [2]

T a b l e

Comparison of experimental and theoretical values of shortite lattice parameters (in Å) at zero pressure

Axis		Lattice constant, Å		Theory-Exp., Å		(Theory- Exp.)/Exp. *100%	
a	Experiment [2]	4.947					
		PBE	LDA	PBE	LDA	PBE	LDA
	Static lattice	5.010	4.845	0.063	-0.102	1.2%	-2.1%
	ZPPE	5.022	4.894	0.075	-0.053	1.5%	-1.1%
	FTPE(298K)	5.035	4.906	0.088	-0.041	1.8%	-0.8%
B	Experiment [2]	11.032					
		PBE	LDA	PBE	LDA	PBE	LDA
	Static lattice	11.151	10.744	0.119	-0.288	1.1%	-2.6%
	ZPPE	11.177	10.858	0.145	-0.174	1.3%	-1.6%
	FTPE (298K)	11.230	10.878	0.198	-0.154	1.8%	-1.4%
C	Experiment [2]	7.108					
		PBE	LDA	PBE	LDA	PBE	LDA
	Static lattice	7.212	6.795	0.104	-0.313	1.5%	-4.4%
	ZPPE	7.251	6.950	0.143	-0.158	2.0%	-2.2%
	FTPE (298K)	7.312	6.990	0.204	-0.118	2.9%	-1.7%

The evolution of the cell parameters (Fig. 2a) shows an anisotropic compression of shortite to be preserved up to 30GPa. Length of *c*-axis varies with pressure much stronger in comparison with the axes *a* and *b*. This difference could be explained by the structural features of shortite. In accordance with the description of the structure adopted in Ref. [2], there are two chains of Ca atoms and (CO_3) groups in the shortite crystal, one oriented along the [011] direction, and another

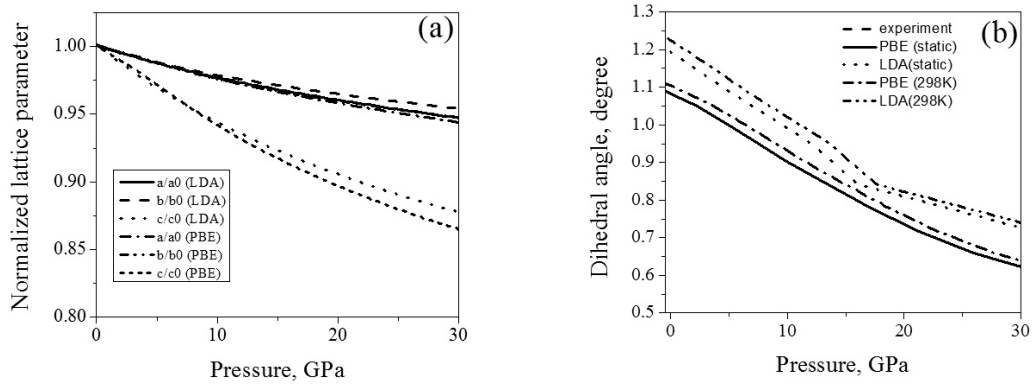

Figure 2. Pressure dependence of the (a) normalized lattice parameters and (b) O-C-O-O dihedral angle

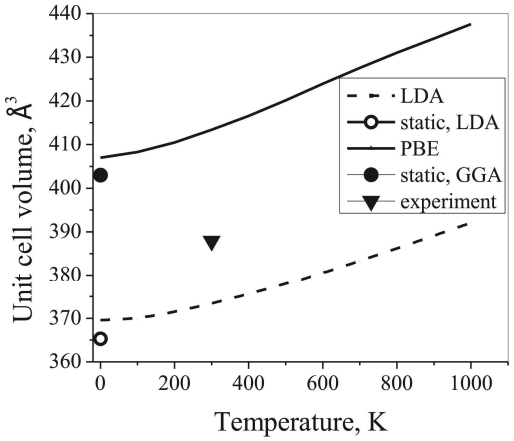

Figure 3. Temperature dependence of unit cell volume at zero pressure

– along the $\left[0\bar{1}1\right]$, while chain of Na atoms and CO_3 groups is oriented parallel to the [001] axis as it is shown in Figure 1a.Under compression, carbonate ions included in the chain of $CaCO_3$ slightly rotated around the ***a*** axis, making structure more compressible along the ***c***-axis. Rotation of carbonate ions is well seen from a comparison of the structures shown in Figure 1a and 1b. Dihedral O-C-O-O angle of carbonate ions in $CaCO_3$ chains also changes under pressure as it is shown in Figure 2b. Calculations show that the dihedral angle decreases with increasing of pressure, making CO_3 groups more planar. (CO_3) groups of $NaCO_3$ chain are planar and preserve planar with pressure. Comparison with experimental data shows that in contrast to the calculation of the lattice constant, dihedral angle is predicted more accurately using PBE than LDA functional.

3.2 Equation of state, thermal expansion and elastic moduli

The equation of state (EOS) *P(V)* for static lattice and in temperature range up to 1000 K using PBE and LDA functionals was calculated in the lattice dynamics approach in quasiharmonic approximation and presented in Figure 4 (a,b). It is seen that *P(V)* at all temperatures are monotonic functions. The effect of temperature causes the uniform shift of the compressibility curve calculated by static lattice EOS except the cases of EOS obtained at sufficiently high temperature using PBE functional. In this case there is a function inflection point in function *P(V)*as it is presented in Figure 4(c). Such behavior results to the features on the bulk modulus as a function of pressure at high temperatures as it is discussed below.

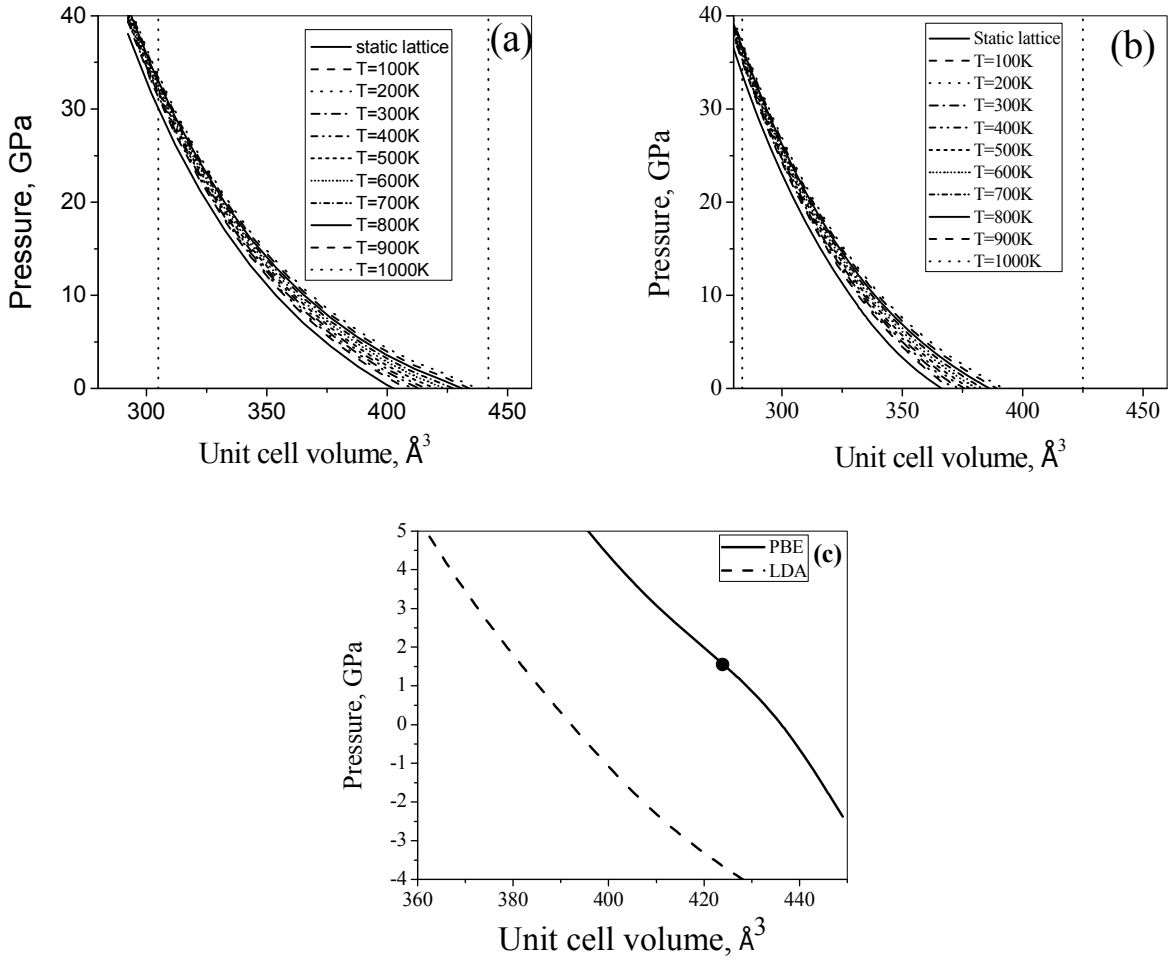

Figure 4. *P-V-T* relations of shortite from *ab initio* calculations using (*a*) PBE and (*b*) LDA functional. Vertical dotted lines show boundaries of mechanical stability for static lattice. (*c*) Equation of state *P(V)* at *T* = 1000 K calculated using PBE and LDA functional. Filled circle indicated the inflection point on PBE obtained dependence *P(V)*

The bulk modulus *B* as a function of temperature *T* up to 1000 K and pressure *P* up to 30 GPA calculated using LDA and PBE functional is shown in Figure 5. LDA calculated values of *B(T)* are approximately 20 % larger than corresponding PBE values. As a function of *T* at given pressure LDA derived bulk modulus

steadily decreases with the temperature. Bulk modulus *T* increases continuously with pressure, i.e. the hardness of shortite decreases with temperature and increases with the applied pressure. PBE calculated value of *B(T)* at zero pressure monotonically decreases at $T < 600$ K and increases at higher temperatures. Bulk modulus is a steadily increasing function of pressure at $T < 600$ K and at higher temperatures it initially decreases with pressure and then increases again. Such non-monotonic behavior is a result of presence of inflection point in the EOS *P(V)*. To understand the origin and physical meaning of this feature, dynamical properties of considered crystal has to be analyzed.

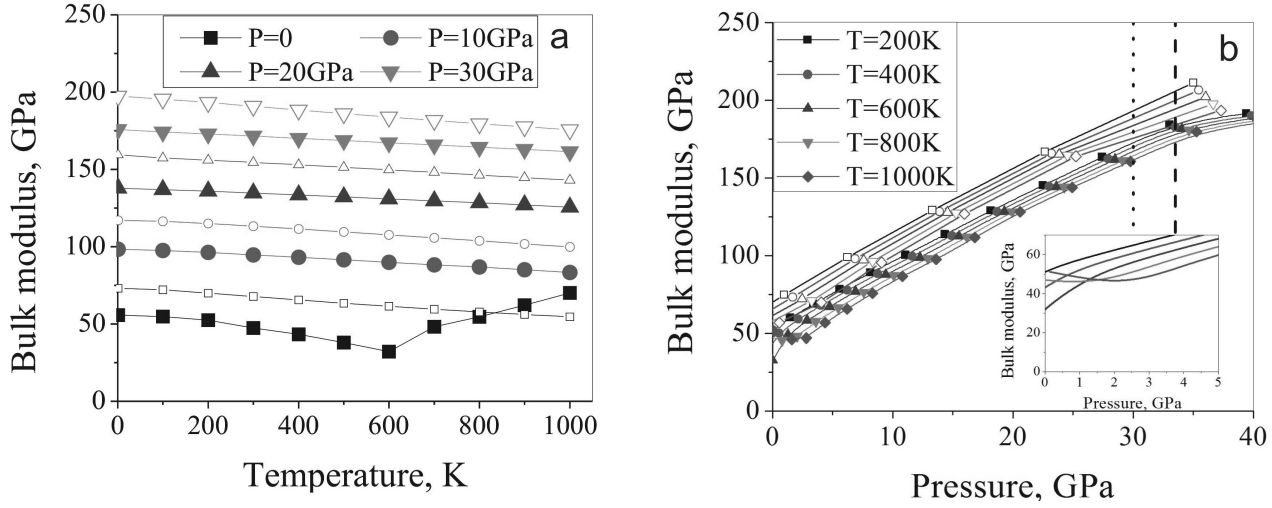

Figure 5. Variations of bulk modulus with temperature (a) and pressure (b) calculated with PBE (closed symbols) and LDA (open symbols) methods. Vertical dashed (dotted) lines represent mechanical stability boundary obtained using PBE (LDA) functional

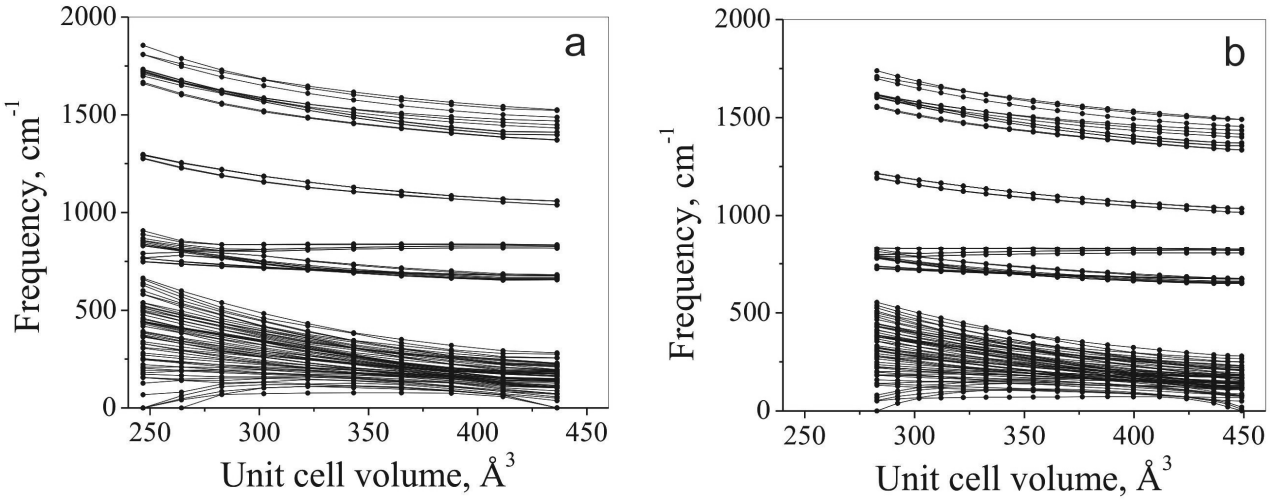

Figure 6. (a) LDA and (b) PBE calculated phonon frequencies of shortite lattice as a function of the unit cell volume

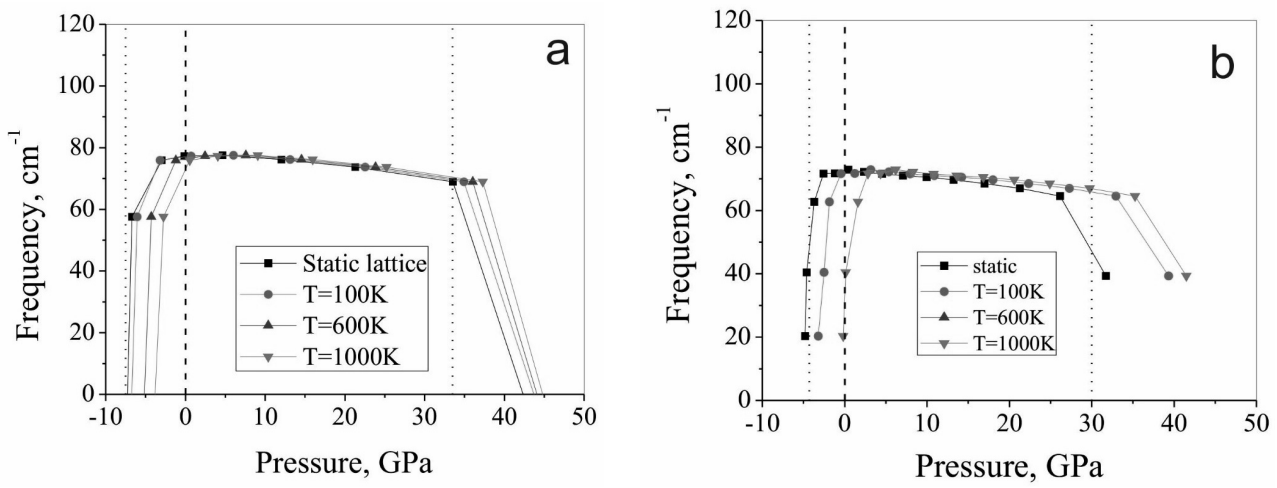

Figure 7. Evolution of the lowest optical vibration mode of shortite lattice with temperature calculated using (a) LDA and (b) PBE methods. Vertical dotted lines represents the mechanical stability boundaries. Dashed lines indicate zero pressure level.

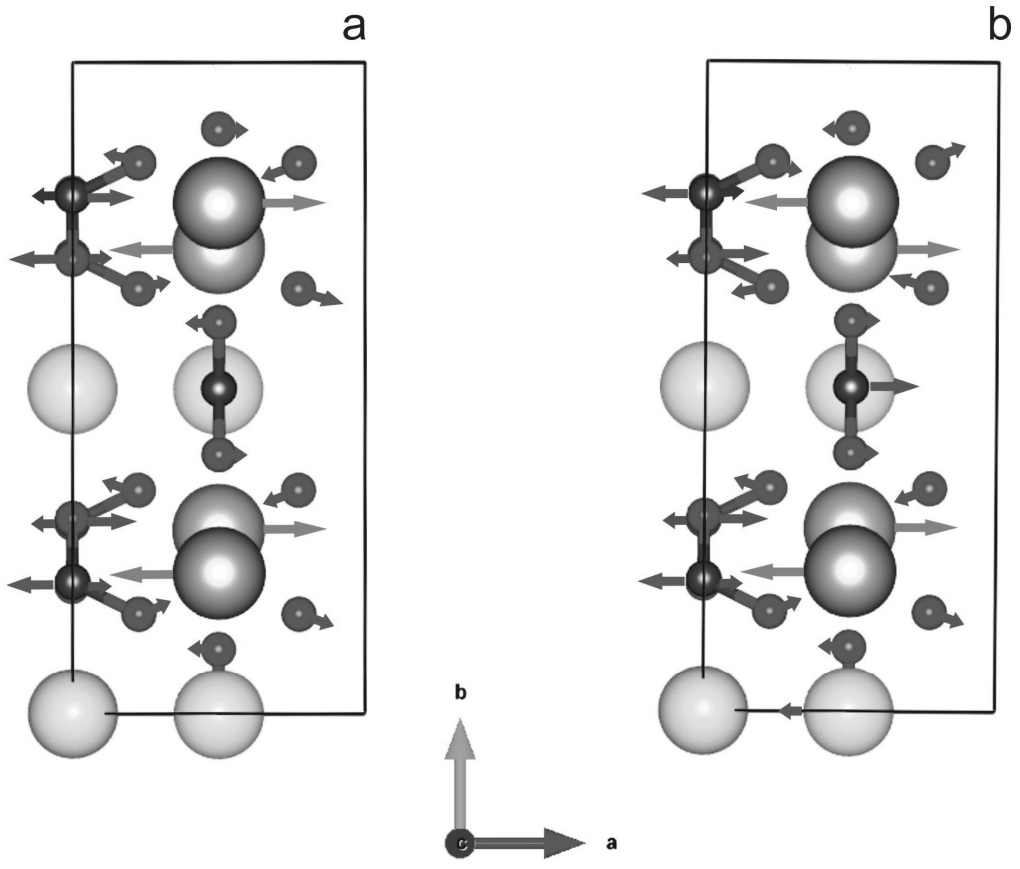

Figure 8. Eigenvectors of the phonons with two lowest frequencies that turns to imaginary values under extremely strong compression and expansion at the Γ-point of Brillouin zone

A fit of the *P-V-T* data to the Vinet-Rydberg and Mie-Grüneisen-Debye equations of state in the pressure range from 298 to 1000 K yields the following thermoelastic parameters for shortite: V_0 = 413.3 Å^3, K_{T0} = 50.1 (1) GPa, K_T' = 5.0, γ = 1.66(1), q = 1.75(3), and θ = 536(40) K. The fit to a HT-VR EOS result in $\partial K_T/\partial T$ = –0.0142(3) GPa/K, and parameters of the coefficient of thermal expansion ($\alpha = a_0 + a_1 T$) are a_0 = 5.2(2) ×10^{-5} K^{-1}, and a_1 = 3.6 (3) ×10^{-8}K^{-2}. If we compare elastic data with previous ones for alkali earth and alkaline-bearing carbonates it is clear that shortite has lower bulk modulus and higher thermal expansion

relative to $CaCO_3$ (agaronite), which has K_{T0} = 66 GPa and α_{298} = 5.2 ×10^{-5} K^{-1}[21], $MgCO_3$ (magnesite) with K_{T0} = 107 GPa and α_{298} = 2.9 ×10^{-5} K^{-1}[22] and $FeCO_3$ (siderite) with K_{T0} = 116 GPa and α_{298} = 2.8 ×10^{-5} K^{-1}[23]. However, rare data for alkali carbonates gives comparable values for bulk modulus ofhigh-pressure polymorph of $K_2Mg(CO_3)_2$(K_{T0} = 50 (7)GPa) and eitelite $Na_2Mg(CO_3)_2$ (K_{T0} = 55 (4)GPa). These values were calculated at K_T' fixed at 5 using VR EOS and unit cell volume data from [5, 24].

Dependence of calculated phonon frequencies on unit cell volume is presented in Figure 6. It can be seen that the phonon spectrum is divided into several bands. The lowest band meets the intermolecular vibrations when the oscillations with higher frequencies intramolecular oscillations carbonate ion. At strong compression as well as at strong tension of crystal lattice the low-frequency optical vibration frequencies tend to zero values and then take imaginary values, that means an absolute dynamic instability of the lattice.

The frequency dependence of the lowest optical vibration depending on the pressure at various temperatures and for static lattice is shown in Figure 7. It can be seen that the dynamic instability of static lattice begins at pressures below about -4 GPa and greater than 30 GPa. With increasing temperature, the pressure boundary of dynamic stability increases. Thus for PBE calculation the dynamic instability, i.e. a sharp reduction in the frequency of the phonon oscillation goes to $P > 0$ at about 600 K. In this case, the phonon frequency, which formally remains positive, but has a small value, at a sufficiently high temperature gives a great contribution to the temperature-dependent part F_{vib} (Eq. 2). With this contribution inflection point appears the equation of state *P(V)*, which leads to the appearance of features in the bulk modulus at low temperatures and high pressures. At sufficiently high pressures, fluctuations with an anomalously low frequency does not contribute to the free energy, which leads to the absence of features in equation of EOS and bulk moduli. An analysis of the eigenvectors (Fig. 8) revealed that the low frequency modes correspond to shear phonons. The transformation of the vibration frequencies in imaginary quantities with volume change indicates the instability of the crystal relative to the corresponding deformation. Summarizing, PBE calculations predict absolute instability of the shortite crystal at low pressures and $T > 600$ K. At the same time, LDA calculations indicate the lattice stability and the experimentally observed instability of the shortite crystal should be caused by its thermodynamic instability, i.e. its Gibbs potential should be larger than the corresponding value for a more stable phase. This means that the accuracy of one or another of used calculation methods is critical, since it indicates a completely different physical cause of the crystal instability.

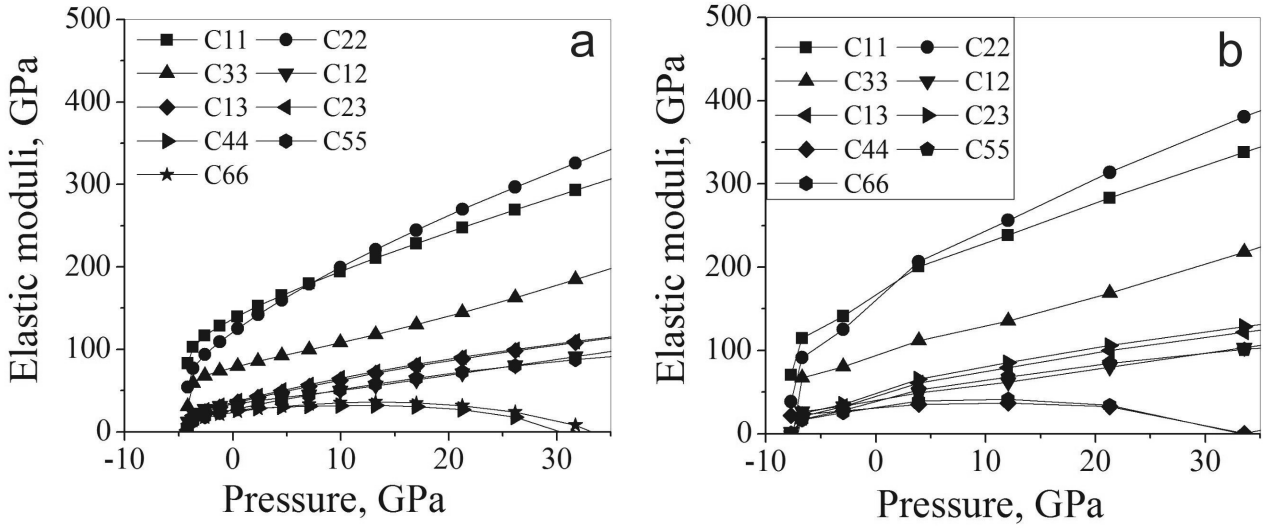

Figure 9. (a) PBE and (b) LDA calculated components of elastic moduli tensor

To determine the limit of absolute stability of the crystal, the tensor of elastic moduli C_{ij} with neglecting the temperature effects was calculated and presented in Figure 9. This approximation corresponds to the low temperature limit. For the mechanical stability of the lattice, all the principal minors of the matrix C_{ij} must be greater than zero. Calculations reveal that all components of elastic moduli tensor, except C_{44} and C_{66}, steadily increases with pressure when $P > 0$. In the negative pressure region, that corresponds to the uniform lattice expansion, all the elastic moduli drastically turn to zero value at $P \approx$ -4.2GPa (PBE) and

–7.5GPa (LDA) andshortite is absolutely unstable at lower pressures. As these pressures currently could not be achieved in experiment, crystal lattice of shortite may exist, at least as a metastable, at any pressures near zero. PBE calculations show that athigh pressureselastic moduli tensor components C_{44} and C_{66} are equal to zero at pressures of 30 and 33 GPa, respectively. Corresponding LDA results predict both C_{44} and C_{66} are equal to zero at pressure of 33.5 GPa. This means that shortite is absolutely unstable at high with respect to shear deformation in the YZ plane or shear deformation YZ and XY, as it follows from PBE and LDA calculations, respectively. As the temperature increases the magnitudes of the elastic moduli of the crystal decrease, the value of the mechanical stability boundary is the upper limit. Experimentally mechanical stability border can be reached at sufficiently low temperatures, when the process of transition to a new thermodynamically more stable phase is complicated due to the slowness of the kinetic processes, as has been observed, for example, for a crystal of ice I_h [25].

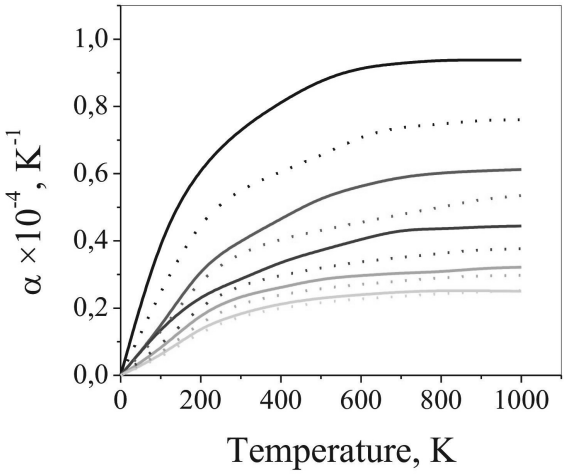

Figure 10. Thermal expansion coefficient α calculated with PBE (solid lines) and L1DA (dotted lines) functionals. Black, red, blue, green, and cyan correspond to external pressure of 0, 5, 10, 15, and 20 GPa, respectively

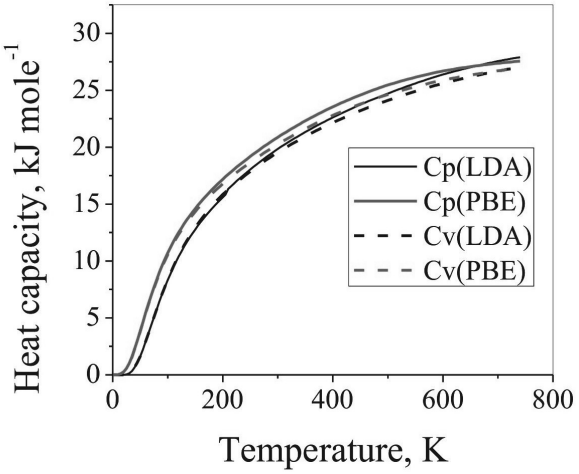

Figure 11. LDA (black lines) and PBE (red lines) calculated heat capacities C_v (dashed lines) and C_p (solid lines) for shortite

Calculated EOS enables us to evaluate the thermal expansion of unit cell at some given external pressure. Temperature dependence of shortite unit cell volumeat zero pressure is shown in Figure10. LDA and PBE calculated unit cell volume values demonstrate similar temperature dependence with systematic deviations from the experimental values as discussed above. Unfortunately, the data in the literature, we found no experimental data on the thermal expansion of the study shortite. Figure 9 shows calculated values of coefficients of thermal expansion at pressures of 0, 5, 10, 15 and 20 GPa using PBE and LDA functionals, correspondingly. The PBE calculated value of thermal expansion coefficient α is approximately 25 % larger than the same value calculated with LDA functional. With increasing pressure difference between LDA and PBE calculated values of α decreases and becomes negligible at pressure 20 GPa. The lattice heat capacity at constant volume and constant pressure using both LDA and PBE functionals was calculated and presented in Figure 11. To our knowledge, there are no published experimental studies of shortitethermal expansion and heat capacity. This information should be extremely important to evaluate the accuracy of used theoretical methods to predict physical properties of Na−Ca double carbonates.

4 Conclusion

In present study theoretical investigation of structural, thermodynamic and dynamic properties of the lattice of shortite $Na_2Ca_2(CO_3)_3$ structure was carried out. The simulation was performed in the framework of the density functional theory in the plane-wave basis using the local density approximation and generalized gradient approximation. Both approaches show good qualitative agreement with the available experimental data. While some properties derived by LDA and PBE methods such as the lattice constants, dihedral O-C-O-O angle of carbonate ions and the values of the elastic moduli of the matrix component C_{ij} exhibit behavior that is typical for the used methods, the results for the equation of state and the bulk modulus are significantly different from each other. This difference is caused by the fact that the dynamic instability during expansion

of shortite crystal lattice in the considered temperature range lies in the region of negative pressure for LDA calculations. For data obtained using PBE functional, dynamic instability occurs at low but positive pressures and $T > 600$ K. In this case soft shear modes give a great contribution to the vibrational part of the free energy that leads to the appearance of the inflection point in the equation of state *P (V)* and lows for the bulk modulus. At the same time, it means that the PBE calculations predict absolute instability of shortite lattice at ambient pressure and $T > 600$ K. LDA calculations indicate that under these conditions crystal is dynamically stable and it decomposition should go through a first order phase transition to more energy favorable phase. To clarify this situation, one need to understand which of theoretical approach is the most accurate that requires a detailed comparison of the calculated data with the experimental results that are not available now.

Acknowledgements

The research was supported by the Russian Foundation for Basic Research through grant (No 14-05-31051) and the Ministry of Education and Science of Russian Federation (MK-3766.2015.15). T.M.I. thanks the Center for Computational Materials Science, Institute for Materials Research, Tohoku University (Sendai, Japan) for their continuous support of the SR16000 M1 supercomputing system. The calculations were performed at supercomputer cluster «Cherry» provided by the Materials Modeling and Development Laboratory at NUST «MISIS» (supported via the Grant from the Ministry of Education and Science of the Russian Federation No. 14.Y26.31.0005). KL thanks to the support from the RF state assignment project No 0330-2016-0006.

References

1 Bolotina N.B. Incommensurately modulated twin structure of nyerereite $Na1.64K0.36Ca(CO_3)_2$. Acta Crystallographica Section B: Structural Science / N.B. Bolotina, P.N. Gavryushkin, A.V. Korsakov, S.V. Rashchenko, Y.V. Seryotkin, A.V. Golovin, B.N. Moine, A.N. Zaitsev, K.D. Litasov, 2017.

2 Dickens B. Crystal structure of $Ca_2Na_2(CO_3)_3$ (shortite). Journal of Research of the National Bureau of Standards — A. Physics and Chemistry / B. Dickens, A. Hyman, W.E. Brown. — 1971. — Vol. 75A.

3 Gavryushkin P. Synthesis and crystal structure of new carbonate $Ca_3Na_2(CO_3)_4$ homeotypic with orthoborates $M_3Ln_2(BO_3)_4$ (M = Ca, Sr, Ba). Crystal Growth & Design / P. Gavryushkin, V. Bakakin, N. Bolotina, A. Shatskiy, Y. Seryotkin, K. Litasov. — 2014. — Vol. 14. — P. 4610–4616.

4 Shatskiy A. Na-Ca carbonates synthesized under upper-mantle conditions: Raman spectroscopic and X-ray diffraction studies / A. Shatskiy, P.N. Gavryushkin, K.D. Litasov, O.N. Koroleva, I.N. Kupriyanov, Y.M. Borzdov, I.S. Sharygin, K. Funakoshi, Y.N. Palyanov, E. Ohtani. European Journal of Mineralogy. — 2015. — Vol. 27. — P. 175–184.

5 Shatskiy A. New experimental data on phase relations for the system Na_2CO_3-$CaCO_3$ at 6 GPa and 900–1400 ºC. American Mineralogist / A. Shatskiy, I.S. Sharygin, K.D. Litasov, Y.M. Borzdov, Y.N. Palyanov, E. Ohtani. — 2013. — Vol. 98. — P. 2164–2171.

6 Gavryushkin P.N. Hydrothermal synthesis and structure solution of $Na_2Ca(CO_3)_2$– «synthetic analogue» of mineral nyerereite. Cryst. Growth Des. / P.N. Gavryushkin, V.G. Thomas, N.B. Bolotina, V.V. Bakakin, A.V. Golovin, Y.V. Seryotkin, D.A. Fursenko, K.D. Litasov, 2016. — Vol. 16. — P. 1893−1902.

7 Blöchl P.E. Projector augmented-wave method, Physical Review B / P.E. Blöchl. — 1994. — Vol. 50. — P. 17953–17979.

8 Kresse G. Efficient iterative schemes for ab initio total-energy calculations using a plane-wave basis set. Physical Review B. / G. Kresse, J. Furthmüller, 1996. — Vol. 54. — P. 11169–11186.

9 Kresse G. From ultrasoft pseudopotentials to the projector augmented-wave method, Physical Review B. / G. Kresse, D. Joubert, 1999. — Vol. 59. — P. 1758–1775.

10 Labat F. Assessing modern GGA functionals for solids, J Mol Model / F. Labat, E. Brémond, P. Cortona, C. Adamo. — 2013. — Vol. 19. — P. 2791–2796.

11 Haas P. Calculation of the lattice constant of solids with semilocal functionals, Phys. Rev. B. / P. Haas, F. Tran, P. Blaha. — 2009. — Vol. 79. — P. 085104.

12 He L. Accuracy of generalized gradient approximation functionals for density-functional perturbation theory calculations. Physical Review B. / L. He, F. Liu, G. Hautier, M.J.T. Oliveira, M.A.L. Marques, F.D. Vila, J.J. Rehr, G.M. Rignanese, A. Zhou. — 2014. — Vol. 89. — P. 064305.

13 Csonka G.I. Assessing the performance of recent density functionals for bulk solids. Phys. Rev. B. / G.I. Csonka, J.P. Perdew, A. Ruzsinszky, P.H.T. Philipsen, S. Lebègue, J. Paier, O.A. Vydrov, J.G. Ángyán. — 2009. — Vol. 79. — P. 155107.

14 Staroverov V.N. Tests of a ladder of density functionals for bulk solids and surfaces. Phys. Rev. B. / V.N. Staroverov, G.E. Scuseria, J. Tao, J.P. Perdew. — 2004. — Vol. 69. — P. 075102.

15 Jackson I. Analysis of P–V–T data: constraints on the thermoelastic properties of high-pressure minerals. Physics of the Earth and Planetary Interiors / I. Jackson, S.M. Rigden. — 1996. — Vol. 96. — P. 85–112.

16 Litasov K.D. Thermal equation of state of superhydrous phase B to 27 GPa and 1373 K / K.D. Litasov, E. Ohtani, S. Ghosh, Y. Nishihara, A. Suzuki, K. Funakoshi Physics of the Earth and Planetary Interiors. — 2007. — Vol. 164. — P. 142–160.

17 Poirier J.P. Introduction to the physics of the Earth's interior, 2nd ed. / J.P. Poirier Cambridge Univ. Press, Cambridge, UK, 2000.

18 Litasov K.D. Thermal equation of state and thermodynamic properties of Molybdenum at high pressure K.D. Litasov, P.I. Dorogokupets, E. Ohtani, Y. Fei, A. Shatskiy, I.S. Sharygin, P.N. Gavryushkin, S.V. Rashchenko, Y.V. Seryotkin, Y. Higo, K. Funakoshi, A.D. Chanyshev, S.S. Lobanov. Journal of Applied Physics. — 2013. — Vol. 113. — P. 093507.

19 Vinet P. Compressibility of solids, Journal of Geophysical Research: Solid Earth / P. Vinet, J. Ferrante, J.H. Rose, J.R. Smith. — 1987. — Vol. 92. — P. 9319–9325.

20 Alchagirov A.B. Energy and pressure versus volume: Equations of state motivated by the stabilized jellium model. Phys. Rev. B. / A.B. Alchagirov, J.P. Perdew, J.C. Boettger, R.C. Albers, C. Fiolhais. — 2001. — Vol. 63. — P. 224115.

21 Litasov K.D. PVT equation of state of $CaCO_3$ aragonite to 29 GPa and 1673 K: In situ X-ray diffraction study / K.D. Litasov, A. Shatskiy, P.N. Gavryushkin, A.E. Bekhtenova, P.I. Dorogokupets, B.S. Danilov, Y. Higo, A.T. Akilbekov, T.M. Inerbaev Physics of the Earth and Planetary Interiors. — 2017. — Vol. 265. — P. 82–91.

22 Litasov K.D. Thermal equation of state of magnesite to 32 GPa and 2073 K. Physics of the Earth and Planetary Interiors / K.D. Litasov, Y.W. Fei, E. Ohtani, T. Kuribayashi, K. Funakoshi. — 2008. — Vol. 168. — P. 191–203.

23 Litasov K.D. P–V–T equation of state of siderite to 33 GPa and 1673 K. Physics of the Earth and Planetary Interiors / K.D. Litasov, A. Shatskiy, P.N. Gavryushkin, I.S. Sharygin, P.I. Dorogokupets, A.M. Dymshits, E. Ohtani, Y. Higo, K. Funakoshi. — 2013. — Vol. 224. — P. 83–87.

24 Shatskiy A. The system K_2CO_3-$MgCO_3$ at 6 GPa and 900-1450°C. American Mineralogist / A. Shatskiy, I.S. Sharygin, P.N. Gavryushkin, K.D. Litasov, Y.M. Borzdov, A.V. Shcherbakova, Y. Higo, K. Funakoshi, Y.N. Palyanov, E. Ohtani. — 2013. — Vol. 98. — P. 1593–1603.

25 Tse J.S. The mechanisms for pressure-induced amorphization of ice Ih. Nature / J.S. Tse, D.D. Klug, C.A. Tulk, I. Swainson, E.C. Svensson, C.K. Loong, V. Shpakov, V.R. Belosludov, R.V. Belosludov, Y. Kawazoe. — 1999. — Vol. 400. — P. 647–649.

Т. Инербаев, П. Гаврюшкин, К. Литасов, Ф. Абуова, А. Ақылбеков

$Na_2Ca_2(CO_3)_2$ шортиттің *P-V-T* күй теңдеуін және темросерпімді қасиеттерін алғашқы қағидалармен зерттеу

Мақалада қосарланған Na-Ca карбонатының құрылымдық, термодинамикалық және динамикалық қасиеттерін теориялық зерттеу тығыздықты функционалдық теориямен жүзеге асырылды. Perdew-Burke-Ernzerhof (PBE) параметрлерінде жергілікті тығыздықты жақындату (LDA) және жалпыланған градиент жақындасу пайдаланылды. Есептелген құрылымдық және серпімділік қасиеттері қолданылған әдістерге тән қасиетті көрсетеді. Сонымен қатар LDA және PBE арқылы алынған *P (V)* және массив модулінің теңдеуі төмен қысымда және жоғары температура кезінде бір-бірінен айтарлықтай ерекшеленеді. Бұл айырмашылық кристалдың динамикалық тұрақсыздығынан туындайды, ол LDA арқылы есептелген шекара әрқашан теріс қысым аймағында жатыр, ал PBE есептеулерінде бұл шама — оң *P (V)* модульдік қасиет. Нәтижелер қолданылатын теориялық әдісінің дәлдігі төмен қысымды торлар тұрақсыздығының төмен қысымда және жеткілікті жоғары температура кезінде түсіну үшін өте маңызды екенін көрсетті.

Кілт сөздер: Na-Ca карбонаты, алғашқы қағидалары, тығыздығын функционалды есептеу, торлы динамика, серпімді модуль, тұрақтылық.

Т. Инербаев, П. Гаврюшкин, К. Литасов, Ф. Абуова, А. Акилбеков

Расчеты из первых принципов уравнения состояния *P-V-T* и термоупругие свойства шортита $Na_2Ca_2(CO_3)_2$

Теоретическое исследование структурных, термодинамических и динамических свойств двойного карбоната $Na_2Ca_2(CO3)_2$ шортита проведено с применением теории функционала плотности. Использовались приближение локальной плотности (LDA) и обобщенное градиентное приближение в параметризации Пердью-Берка-Эрнцерхофа (PBE). Расчетные структурные и эластичные свойства показывают типичное поведение для применяемых методов. В то же время уравнения состояния *P(V)* и величины модуля всестороннего сжатия, полученные с помощью LDA и PBE, существенно отличаются друг от друга при низком давлении и высокой температуре. Это различие обусловлено динамической неустойчивостью кристалла, граница которой, рассчитанная с использованием LDA, всегда лежит в области отрицательного давления, а в случае расчетов PBE этот предел проявляется при положительном давлении, приводящем к особенностям в уравнениях состояния *P(V)* и модуле всестороннего сжатия. Результаты показывают, что точность использованного теоретического метода имеет решающее значение для понимания причины короткой решеточной неустойчивости при низком давлении и достаточно высокой температуре.

Ключевые слова: карбонаты Na-Ca, вычисление функциональных функций первого принципа, динамика решетки, модули упругости, стабильность.